J. Electrochem. Sci. Eng. **14(4)** (2024) 473-486; http://dx.doi.org/10.5599/jese.2135

Open Access : : ISSN 1847-9286
www.jESE-online.org

Original scientific paper

Electrochemical behaviour of Ti6Al4V porous structures fabricated by powder metallurgy route

Maninder Singh[1], Amoljit Singh Gill[1,✉] and Parneet Kaur Deol[2]

[1]*Department of Mechanical Engineering, I. K. Gujral Punjab Technical University, Kapurthala, Punjab, India*

[2]*Department of Pharmaceutics, G.H.G. Khalsa College of Pharmacy Gurusar Sadhar, Ludhiana, Punjab, India*

Corresponding authors: ✉amol_gill@rediffmail.com; Tel.: +91-9988700421

Received: October 16, 2023; Accepted: February 11, 2024; Published: February 21, 2024

Abstract

In this investigation, the powder metallurgy process was used to fabricate porous structures of Ti6Al4V alloy by adding space holder powder particles. The samples were fabricated with varying levels of compaction pressure and other process parameters were kept unchanged in order to investigate the variation in electrochemical behaviour. It was observed that a lower level of compaction pressure resulted in an increase in corrosion current density and rate and a decrease in polarisation resistance. The sample's inability to achieve passivity against electrochemical corrosion, when fabricated using a lower level of compaction pressure, was linked to a higher number of interconnecting micropores. The results of the microstructure analysis confirmed the significant densification of the powder particles when higher compaction pressure was used. The study recommends that a compaction pressure of 300 MPa or higher may be used for fabricating porous structures for biomedical applications.

Keywords

Titanium alloy; biomaterials; space holder; compaction pressure; corrosion

Introduction

The rapid expansion of the biomedical implant sector has contributed to the substantial increase in human life expectancy [1]. This demographic information shows a higher incidence of degenerative ailments, including conditions such as arthritis and osteoporosis [2]. These conditions often result in discomfort or impairment of biological functions. Specifically, there has been a notable increase in primary total hip arthroplasty (THA) and primary total knee arthroplasties (TKA) [3]. Natural bone consists of two main types of hard tissues: cortical bone and cancellous bone. Cortical bone is characterized by its hardness and density, with porosity ranging from 5 to 10% and an elastic modulus ranging from 3 to 30 GPa. On the other hand, cancellous bone is composed of a

spongy network of trabecular bone, exhibiting a much higher porosity of 50 to 90 % and a lower elastic modulus within the range of 0.02 to 2 GPa [4].

The origin of modern implantology can be traced back to the late 19th century. Around this time, significant developments were made in the field. In 1891, researchers experimented with implants constructed from materials such as porcelain and gutta-percha [5,6]. Payne *et al*. took a different approach, using gold-plated tin capsules filled with gutta-percha [7]. However, as mentioned earlier, solid metal implants possess a significantly higher elastic modulus than natural bone. This dissimilarity can lead to a phenomenon known as stress shielding following implantation [8]. Stress shielding, in turn, triggers the dissolution and absorption of the bone tissue that is not under load, potentially causing the implant to become loose over time [9]. Inadequate osseointegration is another concern that hinders the promotion of bone ingrowth and the establishment of a strong bond between the implant and the surrounding bone [10].

Porous metallic structures have gained significant attention in recent years due to their ability to mimic the properties of natural tissues and promote integration within the human body. These structures are intricately designed with interconnected pores that can be customized to attain specific mechanical and biological properties. Such materials hold great promise for biomedical applications, particularly in the development of implants aimed at improving the lives of patients with various medical conditions. Bone implants featuring porous structures prove more effective in preventing subsidence and fostering osseointegration, primarily due to their similarity to the elastic modulus of natural bone [11].

The selection of implant biomaterial stands as a pivotal factor in ensuring the long-term success of implants. The selection of the right implant material is crucial for the success of medical interventions. Each material comes with its advantages and limitations, making it essential to carefully consider the specific application and patient needs. The earliest documented dental implants, crafted from materials like stone and ivory, have historical records tracing back to ancient China and Egypt. Additionally, in the 16^{th} and 17^{th} centuries, dental implants made from gold and ivory were reported [12]. Researchers studied various implant materials and their pivotal role in the success of medical interventions. Various implant materials, including wood, leather, cotton, silk, coral, animal bones, ivory, bitumen, glass, pyrex, bakelite, Formica laminate, and ceramics, have been studied for medical implant applications [13]. However, these early materials exhibited several shortcomings, such as limited durability, low biocompatibility, and restricted availability, rendering them unsuitable for long-term medical use. Consequently, the quest for stable implant materials led to the exploration of metals. Copper and its alloys were initially considered favourable for biomedical applications due to their affordability and bactericidal properties [14]. Nevertheless, they lacked the required durability for load-bearing applications and produced irritant and toxic salts when in contact with the biological environment, making them unsuitable for extended medical use. Other materials like gold, silver, platinum, and ruthenium were also explored but were found to have sufficient irritancy and toxicity to control microbial growth. Researchers also conducted an in-depth examination of the benefits associated with stainless steel [15]. This material is known for its durability, malleability, and compatibility with the human body, presenting an encouraging option. Nonetheless, it faces challenges over time due to its exposure to the body's fluctuating pH levels and corrosive surroundings. Despite the popularity of AISI 316L stainless steel as a preferred alloy for bio-implants, it is essential to note that it may release nickel and chromium, potentially triggering allergic reactions in certain patients. Zinc, a vital element for metabolism, holds promise for various biomedical applications, particularly orthopedic implants and cardiovascular treatments. Yet, its relatively low strength and plasticity pose challenges for long-term

biodegradable applications [16,17]. Cobalt-chromium-molybdenum (CoCrMo) alloys, rich in cobalt, molybdenum, and chromium, gained recognition for their biocompatibility, wear resistance, and corrosion resistance [18]. They found applications in surgical instruments, joint components, and dental prostheses. However, their susceptibility to break during bending and potential immune reactions limits their suitability in certain scenarios. Polymer biomaterials, particularly ultra-high molecular weight polyethylene (UHMWPE), offer inert and biocompatible solutions. Still, wear debris can lead to inflammation and tissue damage [19]. Magnesium, a biodegradable essential element in the human body, holds promise for orthopedic implants. However, its low strength and plasticity present challenges [20].

Titanium, specifically Ti6Al4V, offers an ideal blend of strength, biocompatibility, and corrosion resistance, making it a top choice for various implants [21]. Ti6Al4V excels in mechanical strength, which is particularly important in load-bearing applications. Its corrosion resistance, biocompatibility, and osseointegration capabilities further support its suitability for bio-implants [22,23]. Ti6Al4V, with its outstanding properties and clinical track record, emerges as a preferred choice for bio-implants, contributing to improved patient outcomes and enhanced quality of life [24] and, hence, used for the current investigation.

Fabrication plays a crucial role in customizing desired physical properties, including pore size, interconnectivity for bone ingrowth, and porosity, in implant manufacturing. Various fabrication techniques, such as injecting gas in liquid metal [25], introducing a foaming agent in molten metal [26], indirect foaming technique [26] and powder metallurgy technique [27] have been explored by the researchers to create implants with tailored properties. Space holder-based powder metallurgy process offers cost-effectiveness, enhanced porosity, and parameter control for fabricating porous metallic structures. It follows conventional powder metallurgy principles, employing metallic and space holder materials (*e.g.,* NaCl, boron carbide, saccharose, carbamide, ammonium hydrogen carbonate) to effectively regulate porous structures and improve component efficiency [28]. The mixture of metal powder and space holder powder is compacted to form a green compact. The space holder powder is further removed by the water leaching method or thermal disintegration, leaving behind the final porous metallic structure.

Titanium and its alloys demonstrate remarkable corrosion resistance due to their characteristic of building a protective oxide layer on the surface [29]. The observations made in various studies related to electrochemical corrosion analysis of porous structures of titanium alloys fabricated using the powder metallurgy process are presented in Table 1. Various studies have highlighted the risk of crevice corrosion of titanium structures fabricated using a powder metallurgy process [30-33]. The present study uses a space holder-based powder metallurgy process for fabricating porous structures of titanium alloy Ti6Al4V. Numerous studies have explored the fabrication of porous structures of titanium and its alloys using space holder-based powder metallurgy technique and reported attainment of properties similar to that of natural bone tissue [34]. However, most of these investigations concentrate on the mechanical properties of the porous structures, pore size distribution, and morphology of the emerging porosities. Few reports in the literature look at the variation of corrosion behaviour of porous titanium alloys with powder metallurgy parameters.

The investigation of corrosion is of immense importance. If a metallic implant is susceptible to higher corrosion inside the human body, it will release allergenic, toxic/cytotoxic or carcinogenic elements (*e.g.,* Ni, Co, Cr, V, Al) *in situ*. This will not only burden the body with severe health effects but will also worsen the mechanical qualities of an implant. The resistance of Ti implants against corrosion is highly dependent on the chemical composition of the alloy and the presence of pores [35].

While investigating the effect of the space holder content on the corrosion behaviour of the Ti-16Nb alloy, E Yılmaz *et al.* [36] observed that corrosion resistance got lowered with an increase in space holder content. The effect was attributed to an increase in the porosity of the structures with an increase in space holder content. Compaction pressure has been identified as one of the most significant parameters of the powder metallurgy process that alters the porosity of the fabricated parts [37]. The present study aims to investigate the variation of electrochemical corrosion behaviour of porous structures fabricated using a space holder-based powder metallurgy process by considering compaction pressure as a variable parameter. The study also focuses on identifying the nature of porosity that affects the electrochemical corrosion behaviour of fabricated porous structures.

Table 1. *Observations related to electrochemical corrosion analysis of titanium-based porous structures fabricated using powder metallurgy process*

Titanium alloys	Fabrication process used	Important observations	Ref.
Ti powders	Micro-arc oxidation (MAO) treated samples fabricated using powder metallurgy process	Improved corrosion behaviour has been observed after MAO treatment. Higher improvement was observed in the case of denser samples as compared to porous samples.	[38]
Ti6Al4V/xCu composite	Powder metallurgy	The creation of Ti_2Cu and intermetallic phases during sintering may cause the beneficial impact of adding Cu, which may encourage the formation of a more stable passive layer than that produced by Ti.	[39]
Ti35Nb7Zr5Ta alloy	Powder metallurgy (fully dense and loose sintering)	Electrical impedance values of fully dense β-Ti alloy have been found twice as high as those of commercially pure Ti, and for loose sintered specimens, they were almost five times higher.	[40]
Ti10Mo	Powder metallurgy (porosity variation using space holder content)	With increase in porosity from 2.8 to 66.9 %, the corrosion rate has been found increased exponentially from 1.6 to 17.1 g m^{-2}·day^{-1}.	[41]
TiAg alloys	Powder metallurgy (routes: mechanical alloying (MA) and blended elemental (BE))	The amount and distribution of intermetallic Ti_2Ag in the samples produced with the BE powders have been found directly connected to their superior corrosion resistance compared to the MA samples. The corrosion resistance of TiAg alloys has been found decreased by a significant amount of intermetallics present inside and on the edges of the grains.	[42]
Ti50Ta alloy	Powder metallurgy (variable sintering cycles)	The sintering process longer than 24 h has resulted in more porous and less homogeneous structures. Reduction in resistance to corrosion has been observed at higher sintering temperatures. It has been proposed that the oxide layer developed on the surface of samples fabricated using 24 h sintering cycle was more compact and offered superior corrosion protection than that of the pure Ti.	[43]
Ti35Zr28Nb	Powder metallurgy (porosity variation using space holder content)	With increase in porosity from 51.4 to 64.9 %, the corrosion rate has been found increased from 0.91 to 4.18 μm $year^{-1}$. The porous Ti35Zr28Nb samples demonstrated higher compressive yield strength and decreased corrosion rate as compared to unalloyed Ti samples with almost same porosity.	[44]
Ti40Nb and Ti25Nb5Fe	Powder metallurgy (variable sintering cycles)	For both alloys, samples sintered at 1250 °C for 4 h have demonstrated greater corrosion resistance than samples processed for 2 h.	[45]
Ti6Al4V	Powder metallurgy with halide surface treatment	Halide treatment at 200 °C with NH_4Cl has increased resistance of powder metallurgy sample against corrosion and oxidation at high temperatures.	[46]
Ti16Nb	Powder metallurgy (porosity variation using space holder content)	Corrosion resistance decreased as porosity increased.	[36]

Experimental

A spherical-shaped powder of titanium alloy Ti6Al4V with 99.8 % purity was used to prepare the samples. Ammonium bicarbonate was used as space holder powder because of its easy removal by thermal disintegration during the sintering process. Standard ASTM E-11 was followed to obtain a particle size of 325 mesh of metal powder and 50 mesh of space holder powder using standard sieves [47]. The powder particle size was selected from the literature to match the pore size range favourable for bone growth and vascularization and obtain the required physical strength for bone tissue engineering [48-52].

The porous metallic structures were fabricated using the standard powder metallurgy process consisting of mixing, compaction and sintering. Ti6Al4V powder, ammonium bicarbonate powder and ethanol (2 vol.%, as adhesive) were mixed for 2 h in a rotary mixer to achieve homogeneity. The content of the space holder in the mixture was kept at 30 wt.%. The mixture was further compacted under four distinct uniaxial compaction conditions using a die set and compression testing machine with a crosshead speed of 5 mm min^{-1}. The compacts were then sintered under vacuum conditions (10^{-5} mbar) in a tube furnace. The space holder removal operation was carried out at 200 °C for three hours and the final sintering conditions were fixed at 1200 °C for two hours. The parameters for fabrication of porous structures are summarised in Table 2. As the intended application of these porous structures is load-bearing implants, the selection of the parameters is based upon the recommendations made in various studies (listed in Table 1) to achieve mechanical properties for hard-tissue engineering applications. The fabricated samples were coded as Ti6Al4V-200, Ti6Al4V-300, Ti6Al4V-400 and Ti6Al4V-500 as per the value of used compaction pressure, *i.e*., 200 MPa, 300 MPa, 400 MPa and 500 MPa, respectively.

Table 2. *Parameters for powder metallurgy*

Parameter	Value
Compaction pressure, MPa	200, 300, 400, 500
Ti6Al4V powder particle size, mesh	325
Ammonium bicarbonate particle size, mesh	50
Percentage of *ammonium bicarbonate, w*t.%	30
Sintering temperature, *°C*	*1200*

The fabricated porous samples were polished, degreased in acetone, rinsed with water and air-dried before electrochemical corrosion testing. Phosphate-buffered saline solution (pH of 7.4 at 37°C) (composition: NaCl 8.0 g L^{-1}, KCl 0.2 g L^{-1}, KH_2PO_4 0.24 g L^{-1} and Na_2HPO_4 1.42 g L^{-1}) was considered as electrolyte. As the working, counter, and reference electrodes, respectively, the sample, a platinum wire, and an Ag/AgCl electrode were utilised for electrochemical corrosion testing. The sample was submerged in the electrolyte, and 1800 s of open circuit potentials (OCP) measurements were recorded. A potentiodynamic polarisation test of the sample was carried out after it was submerged in the electrolyte for 30 minutes. Potentiodynamic polarisation curves were captured at a scan rate of 5 mV s^{-1} from -1 to +1 V.

The fabricated samples were analysed using a scanning electron microscope (SEM) for micro-structural analysis. The SEM micrographs of the samples were used to investigate the pore morphology and interconnectivity. Porosity analysis of the porous structures was done using ImageJ software. ImageJ, an open-source image processing tool, plays a vital role in quantifying porosity by effectively separating pores from the material using thresholding and filtering methods. This analytical processing of the SEM micrographs using ImageJ provided the pore structure and porosity

of the samples. The investigation was required to determine the underlying condition of the electrochemical behaviour of the porous structures.

Results and discussion

The manufacturing of porous Ti6Al4V structure offers the possibility of reducing mechanical incompatibility as found in the case of solid components/implants. In addition, the rate at which new bone tissue grows and facilitates bone/implant biological attachment is well-reported for porous structures [53]. However, the main issue with porous metallic structures as implants is their corrosion behaviour [54]. Previous research demonstrated that the amount, form, and distribution of pores had an impact on how well porous materials resist corrosion [33,55]. The body fluid is a complex electrolyte medium that contains several agents, including chloride, that are erosive to metallic implants. Metal ions resulting from degradation by erosion inside the human body may impair the bones' and the surrounding tissues' ability to heal.

The influence of compaction pressure variation in the fabrication of porous metallic structures has been investigated in the context of electrochemical corrosion. The open circuit potential (OCP) curves of Ti6Al4V porous structures fabricated using different levels of compaction pressure as a function of immersion time are shown in Figure 1. The OCP curves of samples Ti6Al4V-500, Ti6Al4V-400 and Ti6Al4V-300 are seen to shift towards positive potential values with increasing time; this behaviour suggests that the oxide is forming on the specimen's surface. These OCP curves closely resemble those displayed by other titanium alloys such as Ti18Nb4Sn [56], Ti30NbXSn [57] and Ti16Nb [36]. Hence, these porous structures follow the titanium alloy typical behaviour of forming a passive protective coating on the exposed surface [58]. The OCP curve for the Ti6Al4V-200 sample shows that with an increase in the soaking period, the potential moved to negative values. A decrease in OCP values represents the dissolvable passive layer, while higher OCP values indicate the creation of a thicker oxide layer [59]. Hence, from the OCP curves of all four samples, it can be determined that the surface passive layer on Ti6Al4V porous structures, fabricated using higher values of compaction pressure, is found to be more stable.

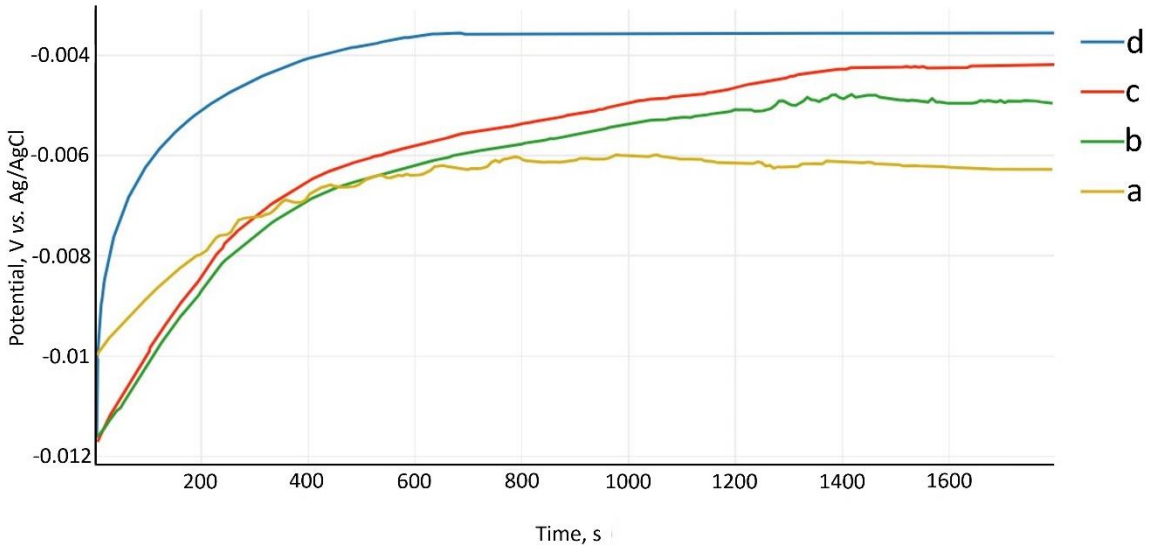

Figure 1. *OCP curves of samples (a) Ti6Al4V-200, (b) Ti6Al4V-300, (c) Ti6Al4V-400 and (d) Ti6Al4V-500*

The electrochemical polarization curves for the four samples are shown in Figure 2. The passivation capabilities of the Ti6Al4V-500, Ti6Al4V-400 and Ti6Al4V-300 porous samples were observed from the anodic polarisation curve. Due to either the heterogeneous structure of the

passive layer that formed on the inner surfaces of the pores or the absence of thickening of the generated passive layer, the Ti6Al4V-200 porous samples did not exhibit a clearly defined passivation plateau. According to Alves *et al*. [60], the rate of passive layer production for inner pores may vary.

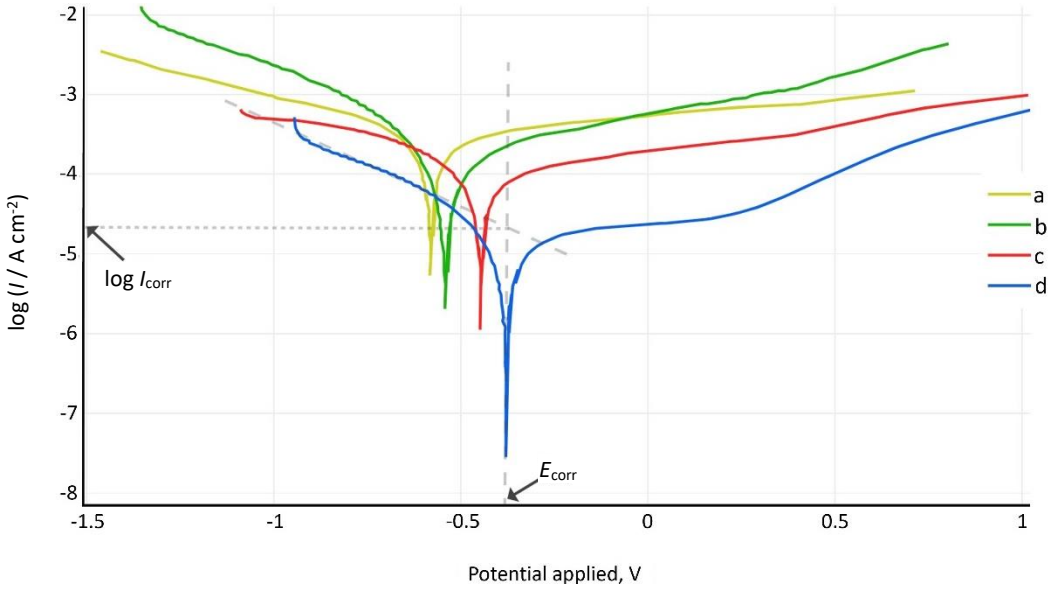

Figure 2. *Potentiodynamic polarization curves of samples (a) Ti6Al4V-200, (b) Ti6Al4V-300, (c) Ti6Al4V-400 and (d) Ti6Al4V-500 (with* E_{corr} *and* I_{corr} *interpretation)*

It is a known fact that porous structures exhibit poorly defined anodic Tafel area due to the dissolution reaction that occurs in the anodic polarisation curves prior to the passivation reaction [61]. Hence, the values of corrosion current density (I_{corr}) are extracted using the Tafel extrapolation method from the cathodic polarisation curves [41,44], as shown for a curve in Figure 2 (curve d).

The values of corrosion potential (E_{corr}) and I_{corr} are enlisted in Table 3. A lower value of I_{corr} and a more positive E_{corr} indicate better anticorrosion performance [62,63]. The findings showed that decreasing compaction pressure causes corrosion resistance to diminish. For powder metallurgy fabricated structures, it is a fact that increased compaction pressure results in increased powder-particle contact area, which lowers porosity [64]. It is possible that the greater surface area of the porous structure is the primary cause of diminished corrosion resistance. According to the reports, porous alloys are more susceptible to corrosion because their large surface area is exposed to the electrolyte [60]. Hence, it is important to investigate the microstructure of the samples.

Table 3. Values of E_{corr} *and* I_{corr} *for samples as per Tafel analysis.*

Sample	I_{corr}, $\mu A\ cm^{-2}$	E_{corr}, V
Ti6Al4V-200	*384*	*-0.58*
Ti6Al4V-300	*301*	*-0.54*
Ti6Al4V-400	*120*	*-0.44*
Ti6Al4V-500	*23*	*-0.36*

SEM pictures of the sintered Ti6Al4V porous structures are shown in Figure 3. The microstructure of the porous sample fabricated using a compaction pressure of 200 MPa (Figure 3(a)) is characterized by loosely packed powder along with large interconnected pores formed by the removal of space holder particles. The pore walls are irregular and indicate relatively poor compaction of metallic powder particles around the space holder powder particle during compaction.

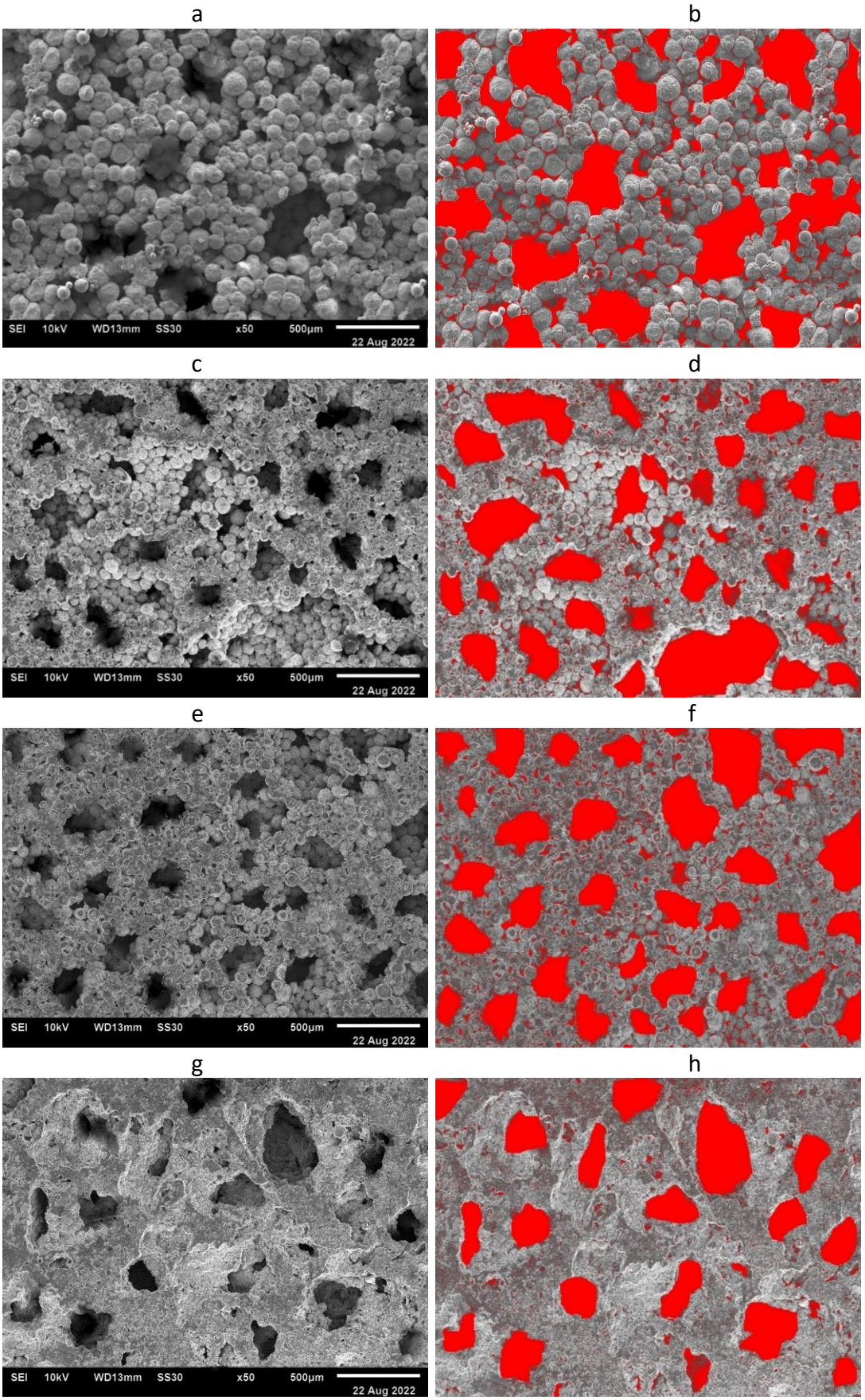

Figure 3. *(a) SEM micrograph of Ti6Al4V-200, (b) 2D image of Ti6Al4V-200 for Porosity analysis, (c) SEM micrograph of Ti6Al4V-300, (d) 2D image of Ti6Al4V-300 for porosity analysis, (e) SEM micrograph of Ti6Al4V-400, (f) 2D image of Ti6Al4V-400 for porosity analysis, (g) SEM micrograph of Ti6Al4V-500, and (h) 2D image of Ti6Al4V-500 for porosity analysis*

Powder-to-powder contact points are less and only a few necking points are visible for a powder particle. As the compaction pressure increases, the difference in powder particle packing is quite distinguishable in Figure 3 (a, c, e and g). With the increase in compaction pressure, the increase in homogeneity of distribution of metal particles around the space holder particle site and the increase in contact points are clearly visible. Figure 3(g) shows the densely packed and effectively sintered metal structure with well-defined pores formed by the thermal disintegration of the space holder.

In order to investigate the nature and distribution of porosity in these samples, the SEM images are further investigated using image processing software, ImageJ. The 2D images of the samples are shown in Figure 3(b, d, f and h). From these images, microporosity and macroporosity in the samples can be confirmed. The presence of microporosity is a characteristic of the powder metallurgy process. However, the macroporosity is deliberately obtained by removing space holder particles. It is evident from Figure 3(b) that in addition to macroporosity, microporosity is present in abundance for sample Ti6Al4V-200. Lower compaction pressure results in an uneven distribution of metal powder particles around the space holder material, leading to a reduced overall powder particle packing. Consequently, uneven distribution and larger pores emerge within the material's structure. Reduction in micro-porosity can be observed in Figure 3 (d, f and h) as the compaction pressure is enhanced. The porous sample fabricated using a compaction pressure of 500 MPa (Figure 3(h)) may be characterized by a significant reduction in microporosity. Also, the micropores are comparatively small and isolated.

From Figure 3 it can be concluded that the increase in compaction pressure leads to a finer and more homogeneous microstructure, resulting in reduced micropore size and the formation of a denser material. Further, a higher level of interconnected porosities in the sample Ti6Al4V-200 and -300 may trap the electrolyte and result in local corrosion. Individual studies by Fojt et al. and Li et al. reported similar observations with other titanium alloys. According to reports, alloys with a high level of interconnected porosity level can create adequate room for electrolyte to be captured and cause crevice corrosion [33,55]. Xie *et al*. [65] highlighted that for porous titanium alloy, the corrosion behaviour is influenced more by the microstructure than by the concentration of the alloying element. Thus, the results indicated that a higher compaction pressure (>300 MPa) must be considered for fabricating porous structures for bone implant applications or other biomedical applications.

Conclusions

This study investigates the effect of compaction pressure on the electrochemical corrosion behaviour of Ti6Al4V porous structures fabricated by the powder metallurgy process. Ti6Al4V is among the Ti alloys most frequently utilised in biomechanical applications (prostheses and implants). Microstructure and pore analysis revealed that both microporosity and macroporosity, as desired for a porous metallic structure for biomedical implant application, can be achieved by powder metallurgy process using the space holder technique. However, with the decrease in compaction pressure lower electrochemical corrosion resistance was observed. The higher level of interconnected micropores in the sample fabricated using a compaction pressure of 200 MPa has been attributed to its inability to attain passivity against electrochemical corrosion. Other levels of compaction pressure (300, 400 and 500 MPa) have shown satisfactory results and may be used for further investigations, which must include investigation of anodic layers formed on the surface of inner pores in terms of homogeneity, composition and morphology in relation to micro- and microporosity is required.

***Conflicts of interest**: The authors declare no conflicts of interest.*

References

[1] S. Tamilselvi, V. Raman, N. Rajendran, Evaluation of corrosion behavior of surface modified Ti-6Al-4V ELI alloy in hanks solution, *Journal of Applied Electrochemistry* **40** (2010) 285-293. https://doi.org/10.1007/s10800-009-9972-5

[2] C. D. Arrieta-González, J. Porcayo-Calderon, V. M. Salinas-Bravo, J. G. Chacon-Nava, A. Martinez-Villafañe. J. G. Gonzalez-Rodriguez, Corrosion behavior of Ni-Cr based coatings in simulated human body fluid environment, *International Journal of Electrochemical Science* **6** (2011) 3644-3655. https://doi.org/10.1016/S1452-3981(23)18277-0

[3] American Joint Replacement Registry, Annual Report on Hip and Knee Arthroplasty Data, 2018. https://www.wavespartnership.org/sites/waves/files/kc/WAVESAnnual-Report-2018-web_0.pdf (accessed 19. 09. 2023)

[4] L. H. Nguyen, N. Annabi, M. Nikkhah, H. Bae, L. Binan, S. Park, Y. Kang, Y. Yang, A. Khademhosseini, Vascularized bone tissue engineering: approaches for potential improvement, *Tissue Engineering B* **18(5)** (2012) 363-382. https://doi.org/10.1089/ten.teb.2012.0012

[5] N. N. Znamenski, Implantation künstlicher zähne, *Deutsche Monatsschrift für Zahnheilkunde* **9** (1891) 87-107.

[6] H. T. Hillischer, Implantation künstlicher Zähne nach dr. Znamensky, *Deutsche Monatsschrift für Zahnheilkunde* **9** (1891) 158-167.

[7] R. E. Payne, Implantation of tin capsule by spreading, *Items of Interest* **14** (1902) 125-226

[8] S. Limmahakhun, A. Oloyede, N. Chantarapanich, P. Jiamwatthanachai, K. Sitthiseripratip, Y. Xiao, C. Yan, Alternative designs of load−sharing cobalt chromium graded femoral stems, *Materials Today Communications* **12** (2017) 1-10. https://doi.org/10.1016/j.mtcomm.2017.05.002

[9] S. Wang, L. Liu, K. Li, L. Zhu, J. Chen, Y. Hao, Pore functionally graded Ti6Al4V scaffolds for bone tissue engineering application, *Materials & Design* **168** (2019) 107643. https://doi.org/10.1016/j.matdes.2019.107643

[10] D. M. D. Ehrenfest, P. G. Coelho, B. S. Kang, Y. T. Sul, T. Albrektsson, Classification of osseointegrated implant surfaces: materials, chemistry and topography, *Trends in Biotechnology* **28(4)** (2010) 198-206. https://doi.org/10.1016/j.tibtech.2009.12.003

[11] C. Song, L. Liu, Z. Deng, H. Lei, F. Yuan, Y. Yang, Y. Li, J. Yu, Research progress on the design and performance of porous titanium alloy bone implants, *Journal of Materials Research and Technology* **23** (2023) 2626-2641. https://doi.org/10.1016/j.jmrt.2023.01.155

[12] C. E. Misch, Contemporary implant dentistry, *Implant Dentistry* **8(1)** (1999) 90. https://journals.lww.com/implantdent/citation/1999/01000/contemporary_implant_dentistry.13.aspx

[13] J. Bartoníček, Early history of operative treatment of fractures, *Archives of Orthopaedic and Trauma Surgery* **130** (2010) 1385-1396. https://doi.org/10.1007/s00402-010-1082-7

[14] S. S. Abdalla, H. Katas, F. Azmi, M .F. M. Busra, Antibacterial and anti-biofilm biosynthesised silver and gold nanoparticles for medical applications: Mechanism of action, toxicity and current status, *Current Drug Delivery* **17(2)** (2020) 88-100. https://doi.org/10.2174/1567201817666191227094334

[15] G. Szczęsny, M. Kopec, D. J. Politis, Z. L. Kowalewski, A. Łazarski, T. Szolc, A review on biomaterials for orthopaedic surgery and traumatology: From past to present, *Materials* **15(10)** (2022) 3622. https://doi.org/10.3390/ma15103622

[16] H. R. Bakhsheshi-Rad, E. Hamzah, H. T. Low, M. Kasiri-Asgarani, S. Farahany, E. Akbari, M. H. Cho, Fabrication of biodegradable Zn-Al-Mg alloy: mechanical properties, corrosion behavior, cytotoxicity and antibacterial activities, *Materials Science and Engineering C* **73** (2017) 215-219. https://doi.org/10.1016/j.msec.2016.11.138

[17] N. El-Mahallawy, H. Palkowski, A. Klingner, A. Diaa, M. Shoeib, Effect of 1.0 wt.% Zn addition on the microstructure, mechanical properties, and bio-corrosion behaviour of micro alloyed Mg-0.24 Sn-0.04 Mn alloy as biodegradable material, *Materials Today Communications* **24** (2020) 100999. https://doi.org/10.1016/j.mtcomm.2020.100999
[18] D. I. Bardos, *Metallurgy of orthopaedic implants* in *Materials Sciences and Implant Orthopedic Surgery,* R. Kossowsky, N. Kossovsky, Eds., Springer, Dordrecht, Netherlands, 1986, p.125. https://doi.org/10.1007/978-94-009-4474-9_11
[19] D. Shekhawat, A. Singh, A. Bhardwaj and A. Patnaik. A short review on polymer, metal and ceramic based implant materials, *IOP Conference Series: Materials Science and Engineering* **1017(1)** (2021) 012038. https://doi.org/10.1088/1757-899X/1017/1/012038
[20] A. Sumayli. Recent trends on bioimplant materials, *Materials Today: Proceedings* **46** (2021) 2726-2731. https://doi.org/10.1016/j.matpr.2021.02.395
[21] J. A. Planell, M. Navarro, *Challenges of bone repair*, in *Bone repair biomaterials*, J. A. Planell, S. M. Best, Eds., Woodhead Publishing Limited, Cambridge, UK, 2009, p.3. https://doi.org/10.1533/9781845696610.1.3
[22] G. A. Sargent, A. P. Zane, P. N. Fagin, A. K. Ghosh, S. L. Semiatin, Low-temperature coarsening and plastic flow behavior of an alpha/beta titanium billet material with an ultrafine microstructure, *Metallurgical and Materials Transactions* A **39** (2008) 2949-2964. https://doi.org/10.1007/s11661-008-9650-y
[23] A. I. Kahveci, G .E. Welsch, Effect of oxygen on the hardness and alpha/beta phase ratio of Ti6A14V alloy, *Scripta Metallurgica* **20(9)** (1986) 1287-1290. https://doi.org/10.1016/0036-9748(86)90050-5
[24] F. Veronesi, P. Torricelli, L. Martini, M. Tschon, G. Giavaresi, D. Bellini, V. Casagranda, F. Alemani, M. Fini, An alternative ex vivo method to evaluate the osseointegration of Ti-6Al-4V alloy also combined with collagen, *Biomedical Materials* **16(2)** (2021) 025007. https://doi.org/10.1088/1748-605X/abdbda
[25] J. Banhart. Manufacture, characterisation and application of cellular metals and metal foams, *Progress in Materials Science* **46(6)** (2001) 559-632. https://doi.org/10.1016/S0079-6425(00)00002-5
[26] J. Banhart, J. Baumeister, Production methods for metallic foams, *MRS Online Proceedings Library* **521** (1998) 121. https://doi.org/10.1557/PROC-521-121
[27] N. Jha, D. P. Mondal, J. D. Majumdar, A. Badkul, A. K. Jha, A.K. Khare, Highly porous open cell Ti-foam using NaCl as temporary space holder through powder metallurgy route, *Materials & Design* **47** (2013) 810-819. https://doi.org/10.1016/j.matdes.2013.01.005
[28] B. Goyal, A. Pandey, Critical review on porous material manufacturing techniques, properties & their applications, *Materials Today: Proceedings* **46** (2021) 8196-8203. https://doi.org/10.1016/j.matpr.2021.03.163
[29] D. Prando, A. Brenna, M. V. Diamanti, S. Beretta, F. Bolzoni, M. Ormellese, M. Pedeferri. Corrosion of titanium: Part 1: Aggressive environments and main forms of degradation. *Journal of Applied Biomaterials & Functional Materials* **15(4)** (2017) e291-e302. https://doi.org/10.5301/jabfm.5000387
[30] K. H. W. Seah and X. Chen, A comparison between the corrosion characteristics of 316 stainless steel, solid titanium and porous titanium, *Corrosion Science* **34(11)** (1993) 1841-1851. https://doi.org/10.1016/0010-938X(93)90021-8
[31] K. H. W. Seah, R. Thampuran, X. Chen, S.H. Teoh, A comparison between the corrosion behaviour of sintered and unsintered porous titanium, *Corrosion Science* **37(9)** (1995) 1333-1340. https://doi.org/10.1016/0010-938X(95)00033-G

[32] K. H. W. Seah, R. Thampuran, X. Chen, S.H. Teoh, The influence of pore morphology on corrosion, *Corrosion Science* **40** (1998) 547-556. https://doi.org/10.1016/S0010-938X(97)00152-2
[33] J. Fojt, L. Joska, J. Málek, Corrosion behaviour of porous Ti-39Nb alloy for biomedical applications, *Corrosion Science* **71** (2013) 78-83. https://doi.org/10.1016/j.corsci.2013.03.007
[34] A. Rodriguez-Contreras, M. Punset, J. A. Calero, F. J. Gil, E. Ruperez, J. M. Manero, Powder metallurgy with space holder for porous titanium implants, *Journal of Materials Science & Technology* **76** (2021) 129-149. https://doi.org/10.1016/j.jmst.2020.11.005
[35] N. Eliaz, Corrosion of metallic biomaterials, *Materials* **12(3)** (2019) 407. https://doi.org/10.3390/ma12030407
[36] E. Yılmaz, A. Gökçe, F. Findik, H. O. Gulsoy, O. İyibilgin, Mechanical properties and electrochemical behavior of porous Ti-Nb biomaterials, *Journal of the Mechanical Behavior of Biomedical Materials* **87** (2018) 59-67. https://doi.org/10.1016/j.jmbbm.2018.07.018
[37] R. Khalifehzadeh, S. Forouzan, H. Arami, S. K. Sadrnezhaad, Prediction of the effect of vacuum sintering conditions on porosity and hardness of porous NiTi shape memory alloy using ANFIS, *Computational Materials Science* **40(3)** (2007) 359-365. https://doi.org/10.1016/j.commatsci.2007.01.007
[38] A. C. Alves, A. I. Costa, F. Toptan, J. L. Alves, I. Leonor, E. Ribeiro, R. L. Reis, A. M. P. Pinto, J. C. S . Fernandes, Effect of bio-functional MAO layers on the electrochemical behaviour of highly porous Ti, *Surface and Coatings Technology* **386** (2020) 125487. https://doi.org/10.1016/j.surfcoat.2020.125487
[39] H. J. Vergara-Hernández, L Olmos, V. M. Solorio, D. Bouvard, J. Villalobos-Brito, J. Chávez, O. Jimenez, Powder Metallurgy Fabrication and Characterization of Ti6Al4V/xCu Alloys for Biomedical Applications, *Metals* **13(5)** (2023) 888. https://doi.org/10.3390/met13050888
[40] L. M. Rodriguez-Albelo, P. Navarro, F. J. Gotor, J. E. de la Rosa, D. Mena, F. J. García-García, A. M. Beltrán, A. Alcudia, Y. Torres, Limits of powder metallurgy to fabricate porous Ti35Nb7Zr5Ta samples for cortical bone replacements, *Journal of Materials Research and Technology* **24** (2023) 6212-6226. https://doi.org/10.1016/j.jmrt.2023.04.212
[41] W. Xu, X. Lu, B. Zhang, C. Liu, S. Lv, S. Yang, X. Qu, Effects of porosity on mechanical properties and corrosion resistances of PM-fabricated porous Ti-10Mo alloy, *Metals* **8(3)** (2018) 188. https://doi.org/10.3390/met8030188
[42] J. Z. Carrullo, A. D. Borrás, V. A. Borrás, J. Navarro-Laboulais, J. P. Falcón, Electrochemical corrosion behavior and mechanical properties of Ti-Ag biomedical alloys obtained by two powder metallurgy processing routes, *Journal of the Mechanical Behavior of Biomedical Materials* **112** (2020) 104063. https://doi.org/10.1016/j.jmbbm.2020.104063
[43] G. Dercz, I. Matuła, M. Zubko, A. Kazek-Kęsik, J. Maszybrocka, W. Simka, J. Dercz, P. Świec, I. Jendrzejewska, Synthesis of porous Ti-50Ta alloy by powder metallurgy, *Materials Characterization* **142** (2018) 124-136. https://doi.org/10.1016/j.matchar.2018.05.033
[44] W. Xu, X. Lu, M.D. Hayat, J. Tian, C. Huang, M. Chen, X. Qu, C. Wen, Fabrication and properties of newly developed Ti35Zr28Nb scaffolds fabricated by powder metallurgy for bone-tissue engineering, *Journal of Materials Research and Technology* **8(5)** (2019) 3696-3704. https://doi.org/10.1016/j.jmrt.2019.06.021
[45] I. Çaha, A. Alves, C. Chirico, A. Pinto, S. Tsipas, E. Gordo, F. Toptan, Corrosion and tribocorrosion behavior of Ti-40Nb and Ti-25Nb-5Fe alloys processed by powder metallurgy, *Metallurgical and Materials Transactions* A **51** (2020) 3256-3267. https://doi.org/10.1007/s11661-020-05757-6
[46] S. A. Tsipas, E. Gordo. A. Jiménez-Morales, Oxidation and corrosion protection by halide treatment of powder metallurgy Ti and Ti6Al4V alloy, *Corrosion Science* **88** (2014) 263-274. https://doi.org/10.1016/j.corsci.2014.07.037

[47] M. P. I. Federation, *Standard test methods for metal powders and powder metallurgy products*, Metal Powder Industries Federation, Princeton, USA, 2019.
[48] Z. Chen, X. Yan, S. Yin, L. Liu, X. Liu, G. Zhao, W. Ma, W. Qi, Z. Ren, H. Liao, M. Liu, Influence of the pore size and porosity of selective laser melted Ti6Al4V ELI porous scaffold on cell proliferation, osteogenesis and bone ingrowth, *Materials Science and Engineering* C **106** (2020) 110289. https://doi.org/10.1016/j.msec.2019.110289
[49] C. M. Murphy, F.J. O'Brien, Understanding the effect of mean pore size on cell activity in collagen-glycosaminoglycan scaffolds, *Cell Adhesion & Migration* **4(3)** (2010) 377-381. https://doi.org/10.4161/cam.4.3.11747
[50] P. Ouyang, H. Dong, X. He, X. Cai, Y. Wang, J. Li, H. Li, Z. Jin, Hydromechanical mechanism behind the effect of pore size of porous titanium scaffolds on osteoblast response and bone ingrowth, *Materials & Design* **183** (2019) 108151. https://doi.org/10.1016/j.matdes.2019.108151
[51] S. Lu, D. Jiang, S. Liu, H. Liang, J. Lu, H. Xu, J. Li, J. Xiao, J. Zhang, Q. Fei, Effect of different structures fabricated by additive manufacturing on bone ingrowth, *Journal of Biomaterials Applications* **36(10)** (2022) 1863-1872. https://doi.org/10.1177/08853282211064398
[52] J. P. Zheng, L. J. Chen, D. Y. Chen, C. S. Shao, M. F. Yi, B. Zhang, Effects of pore size and porosity of surface-modified porous titanium implants on bone tissue ingrowth, *Transactions of Nonferrous Metals Society of China* **29(12)** (2019) 2534-2545. https://doi.org/10.1016/S1003-6326(19)65161-7
[53] N. Abbasi, S. Hamlet, R. M. Love, N.T. Nguyen. Porous scaffolds for bone regeneration. *Journal of Science: Advanced Materials and Devices* **5(1)** (2020) 1-9. https://doi.org/10.1016/j.jsamd.2020.01.007
[54] P. Du, T. Xiang, Z. Cai, G. Xie, The influence of porous structure on the corrosion behavior and biocompatibility of bulk Ti-based metallic glass, *Journal of Alloys and Compounds* **906** (2022) 164326. https://doi.org/10.1016/j.jallcom.2022.164326
[55] Y. H. Li, G. B. Rao, L. J. Rong, Y. Y. Li, The influence of porosity on corrosion characteristics of porous NiTi alloy in simulated body fluid, *Materials Letters* **57(2)** (2002) 448-451. https://doi.org/10.1016/S0167-577X(02)00809-1
[56] F. Rosalbino, D. Maccio, G. Scavino, A. Saccone, In vitro corrosion behaviour of Ti-Nb-Sn shape memory alloys in Ringer's physiological solution, *Journal of Materials Science: Materials in Medicine* **23** (2012) 865-871. https://doi.org/10.1007/s10856-012-4560-3
[57] P. E. Moraes, R. J. Contieri, E. S. Lopes, A. Robin, R. Caram, Effects of Sn addition on the microstructure, mechanical properties and corrosion behavior of Ti-Nb-Sn alloys, *Materials Characterization* **96** (2014) 273-281. https://doi.org/10.1016/j.matchar.2014.08.014
[58] J. Xu, W. Hu, S. Xu, P. Munroe, Z.H. Xie, Electrochemical properties of a novel β-Ta_2O_5 nanoceramic coating exposed to simulated body solutions, *ACS Biomaterials Science & Engineering* **2(1)** (2016) 73-89. https://doi.org/10.1021/acsbiomaterials.5b00384
[59] K. Li, Y. Li, X. Huang, D. Gibson, Y. Zheng, J. Liu, L. Sun, Y.Q. Fu, Surface microstructures and corrosion resistance of Ni-Ti-Nb shape memory thin films, *Applied Surface Science* **414** (2017) 63-67. https://doi.org/10.1016/j.apsusc.2017.04.070
[60] A. C. Alves, I. Sendão, E. Ariza, F. Toptan, P. Ponthiaux, A. M. P. Pinto, Corrosion behaviour of porous Ti intended for biomedical applications, *Journal of Porous Materials* **23** (2016) 1261-1268. https://doi.org/10.1007/s10934-016-0185-0
[61] E. McCafferty. Validation of corrosion rates measured by the Tafel extrapolation method. *Corrosion Science* **47(12)** (2005) 3202-3215. https://doi.org/10.1016/j.corsci.2005.05.046
[62] L. L. Liu, J. Xu, X. Lu, P. Munroe, Z. H. Xie, Electrochemical corrosion behavior of nanocrystalline β-Ta coating for biomedical applications, *ACS Biomaterials Science & Engineering* **2(4)** (2016) 579-594. https://doi.org/10.1021/acsbiomaterials.5b00552

[63] Q. Liu, D. Chen, Z. Kang, One-Step electrodeposition process to fabricate corrosion-resistant superhydrophobic surface on magnesium alloy, *ACS Applied Materials Interfaces* **7(3)** (2015) 1859-1867. https://doi.org/10.1021/am507586u

[64] A. S. Jabur, Effect of powder metallurgy conditions on the properties of porous bronze, *Powder Technology* **237** (2013) 477-483. https://doi.org/10.1016/j.powtec.2012.12.027

[65] F. Xie, X. He, S. Cao, M. Mei, X. Qu, Influence of pore characteristics on microstructure, mechanical properties and corrosion resistance of selective laser sintered porous Ti-Mo alloys for biomedical applications, *Electrochimica Acta* **105** (2013) 121-129. https://doi.org/10.1016/j.electacta.2013.04.105